THE JOURNAL OF BIOLOGICAL CHEMISTRY
Vol. 276, No. 49, Issue of December 7, pp. 45762–45771, 2001
Printed in U.S.A.

Activity of Recombinant Dengue 2 Virus NS3 Protease in the Presence of a Truncated NS2B Co-factor, Small Peptide Substrates, and Inhibitors*

Received for publication, August 2, 2001, and in revised form, September 20, 2001
Published, JBC Papers in Press, October 1, 2001, DOI 10.1074/jbc.M107360200

Donmienne Leung‡, Kate Schroder§, Helen White§, Ning-Xia Fang§, Martin J. Stoermer‡, Giovanni Abbenante‡, Jennifer L. Martin‡, Paul R. Young§, and David P. Fairlie‡¶

From the ‡Centre for Drug Design and Development, Institute for Molecular Bioscience and §Department of Microbiology and Parasitology, School of Molecular and Microbial Sciences, University of Queensland, Brisbane, Queensland 4072, Australia

Recombinant forms of the dengue 2 virus NS3 protease linked to a 40-residue co-factor, corresponding to part of NS2B, have been expressed in *Escherichia coli* and shown to be active against *para*-nitroanilide substrates comprising the P6-P1 residues of four substrate cleavage sequences. The enzyme is inactive alone or after the addition of a putative 13-residue co-factor peptide but is active when fused to the 40-residue co-factor, by either a cleavable or a noncleavable glycine linker. The NS4B/NS5 cleavage site was processed most readily, with optimal processing conditions being pH 9, I = 10 mM, 1 mM CHAPS, 20% glycerol. A longer 10-residue peptide corresponding to the NS2B/NS3 cleavage site (P6-P4′) was a poorer substrate than the hexapeptide (P6-P1) *para*-nitroanilide substrate under these conditions, suggesting that the prime side substrate residues did not contribute significantly to protease binding. We also report the first inhibitors of a co-factor-complexed, catalytically active flavivirus NS3 protease. Aprotinin was the only standard serine protease inhibitor to be active, whereas a number of peptide substrate analogues were found to be competitive inhibitors at micromolar concentrations.

Dengue viruses belong to the flaviviridae family and are transmitted via mosquitoes to millions of people each year in tropical and subtropical regions of the world. They consist of a group of four serologically related viruses referred to as dengue virus types 1–4, with infection resulting in a range of clinical diseases such as dengue fever, dengue hemorrhagic fever, and dengue shock syndrome (1). There is currently no approved vaccine or effective antiviral therapy for these diseases. Like other flaviviruses, the dengue viruses are enveloped with a single, positive sense 11-kilobase RNA genome encoding one long open reading frame. Gene expression involves both co- and post-translational proteolytic processing of a large polyprotein precursor into three structural proteins (C, prM, and E) and seven nonstructural proteins (NS1, NS2A, NS2B, NS3, NS4A, NS4B, and NS5) (Fig. 1*A*) (2). In addition to host proteases, a single virus-encoded protease comprising the amino-terminal 180 amino acids of NS3 (NS3pro) is responsible for cleavage both in *cis* and in *trans* to generate viral proteins that are essential for viral replication and maturation of infectious dengue virions (3). NS3 is at least a trifunctional protein because the carboxyl-terminal region encodes both nucleoside triphosphatase and helicase activities (4, 5).

The dengue virus NS3 protease shares with other flavivirus NS3 proteases a trypsin-like character with a classic serine protease catalytic triad (His^{51}, Asp^{75}, and Ser^{135}) (6–8). Although unlike trypsin it has a marked preference for dibasic residues (*e.g.* Arg and Lys at P1 and P2) and requires the co-factor activity supplied by the nonstructural protein NS2B for efficient catalysis of the proteolytic cleavage of the dengue virus polyprotein (3). The NS2B-NS3 conjugate has been shown to cleave the precursor polyprotein at the NS2A/NS2B, NS2B/NS3, NS3/NS4A, and NS4B/NS5 junctions as well as at internal sites within C, NS2A, NS3, and NS4A (9–11), whereas the host cell proteases, signalase and furin, act on the remaining cleavage sites (Fig. 1*A*) (12–15). Deletion studies employing vaccinia recombinants have further shown that a central 40-amino acid conserved hydrophilic domain within NS2B is sufficient for co-factor activity (16). The flanking hydrophobic residues of NS2B are likely to function by promoting association between the protease complex and infected cell membranes (17). The essential nature of the central hydrophilic domain for proteolytic activity has been recently confirmed *in vitro* with *Escherichia coli* expressed and purified recombinant NS3pro complexed with this NS2B co-factor domain (18).

A therapeutic strategy based on inhibiting proteases (19–21) has precedent in the success of HIV-1[1] protease inhibitors (19, 22, 23), which prevent HIV replication by blocking the viral protease responsible for producing structural and functional HIV proteins in host cells. To mount a similar antiviral program for the dengue viruses, we describe in this paper the expression and purification of two recombinant forms of NS3 protease and the preliminary characterization of the enzymology, including limitations imposed by assay conditions, sub-

* This work was supported in part by the National Health and Medical Research Council of Australia and the Australian Research Council. The costs of publication of this article were defrayed in part by the payment of page charges. This article must therefore be hereby marked "*advertisement*" in accordance with 18 U.S.C. Section 1734 solely to indicate this fact.

¶ To whom correspondence should be addressed. Tel.: 61-7-33651268; Fax: 61-7-33651990; E-mail: d.fairlie@imb.uq.edu.au.

[1] The abbreviations used are: HIV-1, human immunodeficiency virus, type 1; TFA, trifluoroacetic acid; DIPEA, *N*,*N*-diisopropylethylamine; HBTU, *O*-benzotriazole *N*,*N*,*N*′,*N*′-tetramethyluronium hexafluorophosphate; BOP, benzotriazol-1-yloxytris(dimethylamino)phosphonium hexafluorophosphate; DMF, *N*,*N*-dimethylformamide; EtOAc, ethyl acetate; DCM, dichloromethane; THF, tetrahydrofuran; ESMS, electrospray mass spectrometry; pNA, *para*-nitroanilide; HPLC, high pressure liquid chromatography; PCR, polymerase chain reaction; PAGE, polyacrylamide gel electrophoresis; Fmoc, *N*-(9-fluorenyl)methoxycarbonyl; MES, 2-(*N*-morpholino)ethanesulfonic acid; MOPS, 4-morpholinepropanesulfonic acid; CAPS, 3-(cyclohexylamino)propanesulfonic acid; HCV, hepatitis C virus.

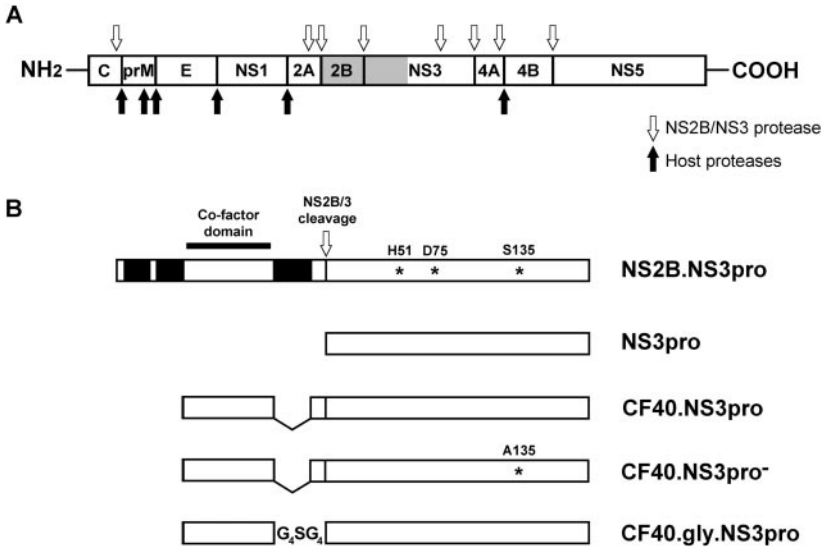

FIG. 1. **Flavivirus polyprotein processing and dengue 2 virus NS3 expression constructs.** *A* shows sites on the flavivirus polyprotein cleaved by host-encoded proteases (*black arrows below*) and the virus-encoded protease complex NS2B.NS3 (*open arrows above*). The NS2B co-factor and the proteolytic domain of NS3 (NS3pro) are *shaded*. *B*, overview of the expression constructs used in this study. The *shading* in *A* corresponds to the first construct and is designated NS2B.NS3pro. Highlighted on this construct in *B* are key features of the protease complex, including the cleavage site (*open arrow*), the catalytic triad of NS3pro (*asterisks*), conserved hydrophobic domains of the NS2B co-factor (*solid boxes*), and the minimum 40-residue co-factor region required for catalytic activity of NS3pro (*solid bar*). The remaining four constructs comprise NS3pro alone (NS3pro), the central 40-amino acid NS2B co-factor domain fused to the 10 amino acids upstream of the NS2B/NS3 cleavage site, the first 184 amino acids of NS3 (CF40.NS3pro), a construct containing a Ser to Ala catalytic triad mutation (CF40.NS3pro$^-$), and a construct comprising the 40-amino acid co-factor domain tethered to NS3pro via a flexible linker (CF40.gly.NS3pro).

strates, and co-factors. We also describe the activity of the first substrate-based peptide inhibitors.

EXPERIMENTAL PROCEDURES

General Methods

Protected amino acids and resins were obtained from Novabiochem. TFA, piperidine, DIPEA, and DMF (peptide synthesis grade) were purchased from Auspep. All other materials were reagent grade unless otherwise stated. Crude peptides were purified by reversed-phase HPLC separations performed on a Waters Delta-Pak reversed-phase C18 preparative column, using a gradient mixture of solvent A (0.1% TFA with water) and solvent B (0.1% TFA, 10% water, and 90% acetonitrile. Analytical HPLC was performed on a Waters system equipped with a 717 plus autosampler, 660 controller, and a 996 photodiode array detector using a reversed-phase C18 (Vydac 201HS5415) column or a reversed-phase protein and peptide column (Vydac 218TP5415). Purified peptides were characterized by analytical HPLC (linear gradient 0–100% solvent B over 30 min) and mass spectrometry. The molecular mass of the peptides was determined by electrospray mass spectrometry recorded on a triple quadrupole (PE SCIEX API III) and electrospray TOF (Applied Biosystems Mariner) mass spectrometers. ^{1}H NMR spectra were recorded on a Varian 300MHz or a Bruker 500MHz NMR spectrometer at 303 K. Proton assignments were determined by two-dimensional NMR experiments (double-quantum filtered correlation spectroscopy, total correlation spectroscopy, and nuclear Overhauser enhancement spectroscopy).

Plasmid Construction

Generation of NS2B.NS3pro PCR product for cloning. C6/36 cells were infected with dengue 2 virus strain NGC at a multiplicity of infection of 1.0 and incubated at 32 °C for 3 days. Infected cell RNA was then extracted with RNazol B (Tel-Test Inc) according to the manufacturer's instructions. cDNA was generated using the NS3proR*Xho*I reverse primer (5′-TATACTCGAGCTATCGAAAAATGTCATCTT-3′; restriction sites are underlined), which was then used as template in a PCR reaction employing this primer and NS2BF*Nco*I (5′-CAAACCATGGCAAGCTGGCCGCTAAATGA-3′). The resulting PCR product comprised the full NS2B sequence and the first 184 amino acids of NS3 (NS3pro) flanked by *Nco*I-*Xho*I sites for cloning into pTM1.

pTM1 Constructs

Four vectors were generated for eukaryotic *in vitro* translation analyses: pTM.NS2B.NS3pro (full-length NS2B.NS3pro), pTM.NS3pro (NS3pro alone), pTM.CF40.NS3pro (NS3pro fused to the 40 amino acid co-factor domain of NS2B), and pTM.CF40.NS3pro$^-$ (containing a mutation in one of the amino acids comprising the NS3pro catalytic triad Ser^{135} to Ala^{135}) (Fig. 1*B*). The NS2B.NS3pro PCR product described above was digested with *Nco*I and *Xho*I and cloned into the pTM1 vector to generate pTM.NS2B.NS3pro. The primers NS3proF*Nco*I (5′-CAAACCATGGCTGGAGTATTGTGGGATGT-3′) and NS3proR*Xho*I were used in a PCR reaction with pTM.NS2B.NS3pro as template. The PCR products were digested with *Nco*I and *Xho*I and cloned into the pTM1 vector to generate pTM.NS3pro. pTM.CF40.NS3pro was generated by amplification of the ligation products of separate PCR reactions. The two PCR products were amplified off the pTM.NS2B.NS3pro template with the primer pairs, CF40F*Nco*I (5′-AGGTACCATGGCCGATTTGGAACTG-3′)/CF40RK*pn*I (5′-GGGGTACCACAGTGTTTGTTCTTCCTC-3′) and NS3proF*Kpn*I (5′-GGGGTACCTGTGGGAAGTGAAGAAACAACGGGCTGGAGTATTGT-3′)/NS3proR*Xho*I. Both PCR products were digested with *Kpn*I, gel-purified, and then ligated. The products of the ligation were then amplified with the outside primers CF40F*Nco*I and NS3proR*Xho*I. The resulting PCR product, comprising the 40-amino acid co-factor domain of NS2B fused to the 10 amino acids immediately upstream of the NS2B-NS3 cleavage site and the first 184 amino acids of NS3pro, was digested with *Nco*I and *Xho*I and cloned into the pTM1 vector. pTM.CF40.NS3pro$^-$ was generated by PCR mutagenesis using pTM.CF40.NS3pro as template and the complementary mutation primers NS3proFS135A (5′-TCTCCTGGAACC**G**CAGGATCTCCAATC-3′) and NS3proRS135A (5′-GATTGGAGATCCTGCGGTTCCAGGAGA-3′) in separate PCR reactions with NS3proR*Xho*I and CF40F*nco*I, respectively. The nucleotide change leading to the S135A mutation is bold type.

pQE9 Constructs

Three vectors were generated for the expression in *E. coli* of amino-terminal His-tagged recombinant dengue viral NS3 protease: pQE9.NS3pro, pQE9.CF40.NS3pro, and pQE9.CF40.gly.NS3pro (CF40 fused to NS3pro via a $Gly_4SerGly_4$ linker). pTM.CF40.NS3pro was used as template for the generation of PCR products with the primer pairs NS3proF*Bam*HI (5′-ATTAGGATCCCTGGAGTATTGTGGGATGT-3′)/NS3proR*Hind*III (5′-GCTAAAGCTTCTATCGAAAAATGTCATCTT-3′) and CF40F*Bam*HI (5′-ATTAGGATCCGCCGATTTAGAACTG-3′)/NS3proR*Hind*III. PCR products were digested with *Bam*HI and *Hin*dIII and cloned into pQE9 to generate pQE9.NS3pro and pQE9.CF40.NS3pro, respectively. pQE9.CF40.gly.NS3pro was generated by overlap PCR using pQE9.CF40.NS3pro as template and the primer pairs CF40F*Bam*HI/CF40glyR (5′-CCCGCCTCCACCACTACCTCCGCCCCCCAGTGTTTGTTCTTCCTC-3′) and NS3proglyF (5′-GGGGGCGGAGGTAGTGGTGGAGGCGGGGCTGGAGTATTGTGGGATG-3′)/

NS3proR*Hind*III to amplify first round PCR products. These were mixed in limiting concentration and then amplified with the outside primers CF40F*Bam*HI and NS3proR*Hind*III. The resulting PCR product, comprising the 40-amino acid NS2B co-factor domain fused to NS3pro via a flexible $Gly_4SerGly_4$ linker, was digested with *Bam*HI and *Hin*dIII and cloned into pQE9. All constructs were confirmed by automated sequence analysis.

Expression and Purification of NS3pro, CF40.NS3pro, and CF40.gly.NS3pro

The pQE9 vector was used for high level, inducible expression of amino-terminal hexahistidine-tagged recombinant proteins. Cultures of *E. coli* strain SG13009, transformed with the corresponding expression plasmids, were grown in 2 liters of LB medium containing 100 μg/ml ampicillin and 25 μg/ml kanamycin at 37 °C until the $A_{600\ nm}$ reached 0.6. The cells were induced for expression by the addition of isopropyl-β-D-thiogalactopyranose to a final concentration of 1 mM and incubated for an additional 3 h at 30 °C. The cells were then harvested by centrifugation, and the pellets were stored at −80 °C until used. For protein purification, the cells were thawed and resuspended in 1 ml of lysis buffer (50 mM HEPES, pH 7.5, 300 mM NaCl, 5% glycerol)/10 ml of original culture. The resuspended cells were lysed by French press or subjected to probe sonication (five 30-s pulses) on ice and then centrifuged at 27,000 × *g* for 30 min at 4 °C. The supernatant was stored at 4 °C or purified immediately by passage through a 2-ml column of Ni^{2+}-nitrilotriacetic acid-agarose (Qiagen) pre-equilibrated with 50 mM HEPES, pH 7.5, containing 300 mM NaCl. The column was extensively washed with buffer containing 20 mM imidazole, and protein was then eluted from the column in buffer containing 100 mM imidazole. Elution fractions were analyzed by 15% SDS-PAGE. Samples of pre- and post-induced cells as well as soluble and insoluble fractions following lysis were collected and also analyzed by 15% SDS-PAGE.

In Vitro Transcription and Translation

An *in vitro* rabbit reticulocyte-coupled transcription/translation system (TnT, Promega) was used to express recombinant protein from the pTM1 vector constructs. The reactions were performed according to the manufacturer's instructions. Briefly, [^{35}S]methionine-labeled protein was expressed by incubation of 0.5 μg of vector DNA with reticulocyte lysate, amino acid (minus methionine) mixture, RNasin, T7 RNA polymerase, and 10.0 μCi of [^{35}S]methionine in a final volume of 25 μl at 30 °C for 90 min. Reactions requiring membranes included 3 μl of canine pancreatic microsomal membranes. The reactions were terminated by the addition of SDS containing gel buffer, and the products were examined by 15% SDS-PAGE and autoradiography.

Peptide Substrates

para-Nitroanilide (pNA) substrates were synthesized by solid phase synthesis (24) using Fmoc protecting groups for the following amino acids: Arg (pmc), Glu (OtBu), Gln (trt), Lys (boc), Ser (tBu), and Thr (tBu). The Fmoc protecting group was removed by shaking the resin with two 1-min treatments with 50% piperidine in dimethylformamide. All amino acids (4 meq) were activated by HBTU (4 meq) and DIPEA (5 meq) in DMF. Couplings were monitored by the quantitative ninhydrin test. All peptides were acetylated with acetic anhydride (20 meq) and DIPEA (10 meq) after the final Fmoc deprotection. Peptide *p*-aminoanilides were assembled on modified chloride trityl resin (substitution value = 0.96 mmol/g) and subsequently cleaved from the solid support with 95% TFA, 2.5% triisopropylsilane, and 2.5% water (15 ml/g resin) for 1 h at room temperature. The respective *p*-aminoanilides were oxidized with oxone (6 meq) in water. Crude peptides were purified by reverse-phase HPLC and lyophilized overnight to give pure *p*-nitroanilides in good yield (50–80%). The 10-residue peptide substrate was assembled on N^{α}-Boc-leucine 4-hydroxymethylphenylacetic acid resin (substitution value = 0.79 mmol/g) (Novabiochem). Protecting groups for individual amino acids were: Arg (Tos), Glu (CHx), and Lys (2-Cl-Z). Removal of the Boc protecting group was effected by shaking the resin twice with 1-min treatments with TFA. All amino acids (4 meq) were activated by HBTU (4 meq) and DIPEA (5 meq) in DMF. Couplings were monitored by the quantitative ninhydrin test. The peptide was deprotected and cleaved from the solid support with liquid HF, *p*-cresol at −5 °C for 1–2 h. Crude peptide was purified by reverse-phase HPLC and lyophilized overnight (30%). Stock solutions of peptides were prepared in water and kept at −80 °C until use. Peptide substrates were Ac-RTSKKR-pNA, Ac-EVKKQR-pNA, Ac-FAAGRK-pNA, Ac-TTSTRR-pNA, and Ac-EVKKQRAGVL-OH corresponding to pNA analogues of the 2A/2B, 2B/3, 3/4A, and 4B/5 cleavage sites and a 10-amino acid segment derived from the 2B/3 site, respectively. Ac-RTSKKR-pNA, retention time (R_t) = 13.5 min, ESMS $[M+H]^+$ = 907.6, $[M+2H]^{2+}$ = 454.3; Ac-EVKKQR-pNA, R_t = 15.3 min, ESMS $[M+H]^+$ = 949.7, $[M+2H]^{2+}$ = 475.3; Ac-FAAGRK-pNA, R_t = 16.7 min, ESMS $[M+H]^+$ = 781.5, $[M+2H]^{2+}$ = 391.3; Ac-TTSTRR-pNA, R_t = 17.7 min, ESMS $[M+H]^+$ = 883.6, $[M+2H]^{2+}$ = 442.3; and Ac-EVKKQRAGVL-OH, R_t = 15.5 min, ESMS $[M+H]^+$ = 1169.4, $[M+2H]^{2+}$ = 585.5.

Protease Assays

A spectrophotometric assay was conducted, using peptide substrates appended to a pNA chromophore, in 96-well plates with each well containing a final volume of 200 μl, an enzyme concentration of 0.5 or 1 μM, and an incubation temperature of 37 °C. Each reaction was monitored continuously by following the increase in A_{405} on a SpectraMax 250 reader. Initial velocities and substrate concentrations were fitted by nonlinear regression to the Michaelis-Menten equation. pH dependence experiments were carried out with the following buffers: MES (pH 5.5–7.0), MOPS (pH 6.5–8.0), Tris (pH 7.5–9.0), ethanolamine (pH 8.5–10.0), and CAPS (pH 10.0–11.5) together with an enzyme concentration of 1 μM, *para*-nitroanilide substrates at 500 μM, and a constant ionic strength (50 mM). For overlapping pH regions, the activity was shown to be unaffected by buffer composition. Buffers included NaCl, glycerol, and detergents varied to optimize assay conditions (see "Results"). Subsequent assays with pNA substrates were performed under optimal conditions that involved 50 mM Tris, pH 9.0, 10 mM NaCl, 20% glycerol, 1 mM CHAPS for a final volume of 200 μl in 96-well plate format and 30 μl for HPLC analysis. Cleavage of the 10-residue peptide substrate was determined by analytical HPLC using a Waters system equipped with a 717 plus autosampler, 660 controller, and a 996 photodiode array detector. The enzyme concentration was 1 μM, the incubation temperature was 37 °C, the incubation time was 2 h (<10% substrate conversion), and the reaction was quenched by addition of 70 μl of 0.1% TFA. Samples of 22.5–90 μl were injected on a Vydac reversed-phase column, and fragments were separated using a 0–100% solvent B gradient at 5%/min. Peak detection was facilitated by monitoring A_{214} and quantified by integration of chromatograms with respect to the appropriate standard peptide. Initial velocities (v) were determined, and kinetic parameters were calculated from weighted nonlinear regression of initial velocities as a function of eight substrate concentrations [S] using GraphPad Prism® software. k_{cat}/K_m values were calculated assuming Michaelis-Menten kinetics, $v = V_{max}[S]/([S] + K_m)$. Quadruplicate measurements were taken for each data point. The data are reported as the means ± S.E.

Inhibitor Assay

General protease inhibitors were used to confirm the presence of a serine protease. Inhibitors were assayed in a 96-well plate format using 50 mM Tris, pH 9.0, 10 mM NaCl, 20% glycerol, 1 mM CHAPS in a final volume of 200 μl. Typically CF40.NS3pro (0.5 μM) was preincubated with various concentrations of test compounds at 37 °C for 10 min. The reaction was initiated by the addition of substrate Ac-TTSTRR-pNA at 500 μM. On the other hand the peptidic inhibitors were assayed using CF40.gly.NS3pro (0.5 μM) in a 96-well plate format using 50 mM HEPES, pH 7.5, 50 mM NaCl, 20% glycerol, 1 mM CHAPS in a final volume of 200 μl. Typically these test compounds were incubated with the enzyme conjugate at 37 °C for 50 min, and then substrate cleavage was initiated by the addition of the chromogenic substrate Ac-TTSTRR-pNA at 500 μM. Reaction progress was monitored continuously by following the increase in A_{405} on a SpectraMax 250 plate reader. IC_{50} values were determined for inhibitors from substrate titration experiments performed in the presence of increasing inhibitor concentration using Dixon plots (1/v *versus* [I]). K_i values were calculated from IC_{50} values according to the equation, $K_i = IC_{50}/(1 + S/K_m)$. Triplicate measurements were taken for each data point. The data are reported as the means ± S.E.

Peptide Inhibitors

α-Keto Amide Inhibitors (1–3)—Inhibitors **1** (Ac-FAAGRR-{CO-CONH}-SL-$CONH_2$), **2** (Ac-TTSTRR-{COCONH}-SL-$CONH_2$), and **3** (Ac-TTSTRR-{COCONH}-GTGN-$CONH_2$) were synthesized on 4-methylbenzhydrylamine resin (substitution value = 0.59mmol/g). The peptides were assembled by stepwise solid phase synthesis using the Boc protocol. Protecting groups for individual amino acids were: Arg (Tos), Ser (Bzl), and Thr (Bzl). Removal of the Boc protecting group was effected by shaking the resin twice with 1-min treatments with TFA. All amino acids (4 meq) were activated by HBTU (4 meq) and DIPEA (5 meq) in DMF with the exception of Boc-Arg(Tos)-α-hydroxy acid (2

meq), which was activated with PyBOP (2 meq) and DIPEA (3 meq) in DMF. Couplings were monitored by the quantitative ninhydrin test. All peptides were acetylated using activated acetic acid with HBTU/DIPEA in DMF after the final Boc deprotection. The α-hydroxyl moiety was oxidized on resin with Dess Martin Periodinane (2 meq) in dry Me_2SO for 2 h at room temperature to give the desired α-keto amides. The inhibitors were deprotected and cleaved from the solid support with liquid HF, *p*-cresol at −5 °C for 1–2 h, during which time partial racemization occurs at P1 arginine, producing a mixture of two diastereoisomers. These α-keto amides are also unstable in basic solutions. Crude peptides were purified by reversed-phase HPLC and characterized by analytical HPLC and electrospray mass spectrometry. Analytical HPLC (gradient, 0–100% solvent B over 30 min): 1, R_t = 16.1 min, ESMS $[M+H]^+$ = 946.8, $[M+2H]^{2+}$ = 473.9; 2, R_t = 14.1 min, ESMS $[M+H]^+$ = 990.8, $[M+2H]^{2+}$ = 495.9; 3, R_t = 12.2 min, ESMS $[M+H]^+$ = 1119.6, $[M+2H]^{2+}$ = 560.3.

Synthesis of Boc-Arg(Tos)-α-hydroxy Acid—Boc-Arg(Tos)-OH was activated with BOP/DIPEA in DCM and reacted with *N*-methyl-*O*-methylhydroxylamine hydrochloride to give the Weinreb amide in a yield of 81%. The amide was reduced with $LiAlH_4$ in THF at 0 °C, giving the aldehyde in good yield (99%). The aldehyde was treated with KCN to generate the cyanohydrin, which was partially purified by passage through a short column of silica and treated directly with concentrated HCl at room temperature for 3 days. Subsequent neutralization to pH 6 gave the unprotected α-hydroxy acid as colorless crystals (53%). The α-hydroxy acid could be protected at the amino terminus as the Boc or Fmoc derivative by using either Boc-carbonate or Fmoc-OSu in basic solution under standard conditions (66%).

Boc-Arg(Tos)-NMeOMe—Boc-Arg(Tos)-COOH (10.0 g, 23.4 mmol) and *N*-methyl-*O*-methyl-hydroxylamine hydrochloride (2.27 g, 23.4 mmol) were dissolved in DCM (50 ml). BOP (10.3 g, 23.4 mmol) and DIPEA (12.2 ml, 70.2 mmol) were added to the stirred mixture and allowed to react for 45 min at room temperature. To this solution was added 10% $KHSO_4$ solution (20 ml), and the mixture was extracted with DCM (3 × 50 ml). The organic layers were combined and washed with 10% $KHSO_4$ (2 × 50 ml), saturated $NaHCO_3$ (3 × 50 ml), water (3 × 50 ml), and brine (3 × 50 ml). The organic layer was dried with $MgSO_4$ and concentrated *in vacuo* to yield product as an oil, which was triturated with a small volume of ethyl acetate (20 ml) to give a white powder. The powder was filtered and dried (9.0 g, 81%). ESMS $[M+H]^+$ = 472.3; ^1H NMR ($CDCl_3$) δ 7.77 (d, 2H, Ar-H), 7.23 (d, 2H, Ar-H), 6.55 (br.s, 2H, NH), 5.56 (d, 1H, Boc-NH), 4.62 (m, 1H, αCH), 3.72 (s, 3H, O-Me), 3.36 (m, 1H, γCH), 3.20 (s, 3H, N-Me), 3.18 (m, 1H, δCH), 2.40 (s, 3H, Ar-CH_3), 1.64 (m, 4H, βCH_2 and γCH_2), 1.42 (s, 9H, Boc).

Boc-Arg(Tos)-CHO—Boc-Arg(Tos)-NMeOMe (15.0 g, 31.8 mmol) was dissolved in anhydrous THF (200 ml) and stirred under argon at 0 °C. $LiAlH_4$ (2.0 g, 31.8 mmol) was added in small portions and stirred for 1 h at 0 °C. The reaction mixture was poured into 10% $KHSO_4$ solution (100 ml) and extracted with EtOAc (3 × 100 ml). The organic layers were combined and washed with 10% $KHSO_4$ (3 × 100 ml), water (3 × 100 ml), and brine (3 × 100 ml). The EtOAc layer was dried with $MgSO_4$ and concentrated *in vacuo* to yield product as white powder (13.0 g, 99%). The aldehyde was not purified further but used directly in subsequent transformations. ESMS $[M+H]^+$ = 413.2; ^1H NMR ($CDCl_3$) δ 7.74 (d, 2H, Ar-H), 7.25 (d, 2H, Ar-H), 6.79 (br.s, 1H, NH), 5.66 (s, 1H, aminol-CH), 5.23 (br.s, 1H, NH), 5.05 (d, 1H, Boc-NH), 3.5–3.75 (br.m, 2H, αCH, and δCH), 3.14 (m, 1H, δCH) 2.40 (s, 3H, Ar-CH_3), 1.45–1.80 (m, 4H, βCH_2, and γCH_2), 1.41 (s, 9H, Boc).

H-Arg(Tos)-α-hydroxy Acid—Boc-Arg(Tos)-CHO (13.0 g, 31.4 mmol) was dissolved in EtOAc (65 ml). KCN (3.54 g) was dissolved in 1:1 mixture of methanol and water (70 ml) and added to the aldehyde. The homogenous reaction mixture was stirred overnight. The mixture was diluted with water (50 ml), and the organic layer was washed with water (3 × 100 ml). The EtOAc layer was dried with $MgSO_4$ and concentrated *in vacuo* to an orange oil that was passed through a short column of silica (30% EtOAc/hexane eluant) to remove base-line material. The resultant oil hydrolyzed with concentrated HCl (60 ml) at room temperature for 3 days. The solution was reduced to dryness, redissolved in water (60 ml), and neutralized to pH 6 with 2 M NaOH solution. The desired product existed as two diastereoisomers and precipitated as colorless crystals (6.0 g, 53%). ESMS $[M+H]^+$ = 359.2.

Boc-Arg(Tos)-α-hydroxy Acid—H-Arg(Tos)-α-hydroxy acid (0.81 g, 2.3 mmol) was dissolved in 1:1 THF/water (10 ml). 2 M NaOH solution (2.3 ml, 4.5 mmol) was added, and the reaction was cooled to 0 °C. Boc-carbonate (0.74 g, 3.4 mmol) was added and stirred for 1 h at 0 °C. The reaction was allowed to warm to room temperature and stirred overnight. THF was removed *in vacuo*, and the residue was diluted with water (10 ml). The basic aqueous layer was extracted with EtOAc (3 × 30 ml). The aqueous layer was subsequently acidified with 10% $KHSO_4$ (20 ml) and extracted with EtOAc (3 × 30 ml). The organic layer was washed with water (3 × 50 ml), dried with $MgSO_4$, and concentrated *in vacuo* to yield product as a white solid (0.68 g, 66%). ESMS $[M+H]^+$ = 459.3. ^1H NMR ($CDCl_3$) (The two diastereomeric products had coincident NMR spectra; only the two Boc signals at δ 1.40, 1.43 were resolved) δ 7.5 (m, 4H, Ar-H), 7.22 (m, 4H, Ar-H), 6.35 (m, 4H, εNH + ωNH), 5.20 (m, 2H, BocNH), 4.67 (m, 2H, CH), 4.00 (m, 2H, αCH), 3.18 (m, 4H, δCH_2), 2.38 (s, 6H, CH_3), 2.27 (m, 6H, OH + COOH + NH), 1.54 (m, 8H, βCH_2 + γCH_2), 1.43 (s, 9H, Boc), 1.40 (s, 9H, Boc).

Arginal Inhibitor (4)—The method developed for the synthesis of Ac-FAAGRR-CHO (**4**) is a modification of the Corvas procedure (25–28) and used arginine protected as the cyclol synthon. Our modifications to the literature procedure entailed the use of phosphonium coupling reagents instead of mixed anhydride methods and of more strongly acidic solvent for the hydrogenolysis of the nitro guanidine protecting group. Instead of assembling short arginals as reported (25–28), we utilized solid phase peptide synthesis to assemble the pentapeptide Ac-FAAGR-COOH, which was then coupled in solution to the cyclol.

Ac-FAAGR-OH—The pentapeptide acid was assembled by standard manual Fmoc solid phase peptide synthesis using Novabiochem Fmoc-Arg(pmc)-Wang resin (substitution value = 0.54 mmol/g) as described above. HRMS calculated for $C_{25}H_{38}N_8O_7$ $[M+H]^+$ =563.2936, found 563.2935. ^1H NMR (Me_2SO-d_6) δ 8.18 (d, 1H, AlaNH), 8.15 (t, 1H, GlyNH), 8.12 (d, 1H, PheNH), 8.03 (d, 1H, ArgNH), 8.02 (d, 1H, AlaNH), 7.59 (bs, 1H, Arg-εNH), 7.4–6.8 (bs, 4H, NH_2 + NH_2), 7.24 (m, 4H, Ar-H), 7.17 (m, 1H, Ar-H), 4.50 (m, 1H, PheαCH), 4.28 (m, 1H, AlaαCH), 4.25 (m, 1H, AlaαCH), 4.22 (m, 1H, ArgαCH), 3.74 (m, 2H, GlyαCH), 3.32 (bs, 1H, COOH), 3.10 (m, 2H, Arg δCH_2), 3.00 (m, 1H, Pheβ CH), 2.73 (m, 1H, Pheβ CH), 1.78–1.49 (m, 4H, Arg βCH_2 + Arg γCH_2), 1.73 (s, 6H, CH_3).

N-α-Boc-N-ω-nitroarginine Lactam—To a stirred suspension of *N*-α-Boc-*N*-ω-nitroarginine (6.38 g, 20 mmol) and BOP (9.72 g, 20 mmol) in THF (120 ml) was added DIPEA (10.4 ml, 60 mmol), and the solution was stirred at room temperature overnight. The solvent was removed under vacuum, and the residue was partitioned between EtOAc (400 ml) and hydrochloric acid (1 M, 200 ml). The organic extract was washed with hydrochloric acid (1 M, 2 × 200 ml), dried with $MgSO_4$, filtered, and evaporated to yield the crude product as a yellow foam. Column chromatography (10% EtOAc/DCM) yielded pure product (3.01 g, 50%) as a white foam. ESMS $[M+H]^+$ = 302.1. ^1H NMR ($CDCl_3$) δ 10.40 (bs, 1H, NH), 9.53 (bs, 1H, NH), 5.15 (m, 1H, BocNH), 4.65 (m, 1H, δCH), 4.46 (m, 1H, δCH), 3.56 (m, 1H, αCH), 2.48 (m, 1H, βCH), 1.95 (m, 2H, γCH_2), 1.63 (m, 1H, βCH), 1.48 (m, 9H, Boc).

N-α-Boc-N-ω-nitroargininal Ethyl Cyclol—To a stirred solution of $LiAlH_4$ in THF (1.0 M, 10 ml, 10 mmol) cooled in an ice bath was added dropwise EtOAc (1.13 ml, 10 mmol) in THF (5 ml). The solution was stirred for 30 min at 0 °C and treated with a solution of *N*-α-Boc-*N*-ω-nitro-L-arginine lactam (3.01 g, 10 mmol) in THF (15 ml). The mixture was stirred for 30 min at 0 °C and treated with a mixture of hydrochloric acid (1 M, 3 ml) and THF (3 ml) dropwise, followed by hydrochloric acid (1 M, 60 ml) at room temperature. The solution was extracted with EtOAc (3 × 60 ml), washed with saturated $NaHCO_3$ (15 ml), brine (20 ml), dried with $MgSO_4$, filtered, and evaporated to yield the crude aldehyde as a white foam. ESMS $[M+H]^+$ = 304.2. The crude aldehyde was dissolved in ethanol (15 ml), and concentrated HCl (50 μl) was added. The mixture was stirred at room temperature for 7 h, and the solvent was removed under vacuum. The crude product was purified by column chromatography (0–10% EtOAc/DCM to yield 1.72 g (52%) of the title compound as a white foam. ESMS $[M+H]^+$ = 332.2.

N-ω-Nitroargininal Ethyl Cyclol.TFA—N-α-Boc-*N*-ω-Nitroargininal ethyl cyclol (1.72 g, 5.2 mmol) was treated with 50% TFA/DCM (5.6 ml) for 10 min. The solution was added dropwise to diethyl ether (50 ml) with swirling. The product was collected at the pump, washed briefly with diethyl ether (3 × 100 ml), and dried under vacuum to yield pure product (1.13 g, 63%). ESMS $[M+H]^+$ = 232.1. ^1H NMR (Me_2SO-d_6) δ 8.74 (bs, 1H, NH), 8.05 (bs, 1H, NH), 5.93 (m, 1H, CH), 3.74 (m, 1H, δCH), 3.51 (m, 1H, 1/2 of CH_2), 3.45 (m, 1H, 1/2 of CH_2), 3.32 (m, ^3H, NH_3), 3.27, (m, 1H, αCH), 3.03 (t, 1H, δCH), 1.76 (m, 3H, βCH_2 + γCH), 1.55 (m, 1H, γCH), 1.19 (t, 3H, CH_3).

Ac-FAAGR-ω-nitroarginal Ethyl Cyclol—To a stirred solution of Ac-FAAGR-OH (30.4 mg, 0.054 mmol), BOP (22 mg, 0.05 mmol), and cyclol TFA salt (31 mg, 0.09 mmol) in DMF (1.5 ml) was added DIPEA (39 μl, 5 meq). The mixture was stirred at room temperature for 3 h, and the solvent was removed under reduced pressure. The residue was purified by preparative HPLC (gradient: 0–100% B over 50 min, R_t = 12.5 min) to yield the product as a white powder. ESMS $[M+H]^+$ = 776.6.

Ac-FAAGR-arginal Ethyl Cyclol—To a solution of the above nitroarginal ethyl cyclol in a mixture of water (1 ml), ethanol (1 ml), and

acetic acid (glacial, 15 ml) was added palladium-on-carbon catalyst (10%, 30 mg), and the mixture was hydrogenated in a Parr apparatus at 45 p.s.i. H_2 for 48 h. The mixture was filtered through Celite and washed with water, and the solvent was removed under reduced pressure to yield the product as a colorless residue. ESMS $[M+H]^+ = 731.4$.

Ac-FAAGR-arginal (4)—A solution of the above arginal ethyl cyclol in water (5 ml) was cooled in an ice bath and treated with hydrochloric acid (10 M, 45 μl). The reaction was monitored by mass spectrometry and when complete (2.5 h) was quenched by the addition of sodium acetate solution (2.5 M, 1 ml). The solution was filtered, and the product was purified by preparative HPLC (gradient: 0–100% solvent B over 50 min, $R_t = 9.1$ min) to yield the product as a white powder. The ^{1}H NMR spectrum of the aldehyde in water showed three sets of resonances (4:1:1 ratio) attributable to the two diastereomeric closed aminol forms and one open chain hydrate form of the aldehyde. HRMS calculated for $C_{31}H_{50}N_{12}O_8$ $[M+H]^+ = 703.3998$, found = 703.3989.

RESULTS

In Vitro Expression of Catalytically Active NS3pro—The first aim of this study was the expression and purification of a catalytically active recombinant dengue virus NS3 protease, initially for use in *in vitro* based assays. To confirm that the sequences we derived by reverse transcription-PCR from a dengue virus-infected cell RNA encoded an active protease, we first expressed these recombinant proteins in a rabbit reticulocyte-coupled transcription/translation system (Fig. 2*A*). pTM.NS2B.NS3pro encodes the NS2B gene, which is an essential co-factor for proteolytic activity, fused to the first 184 amino acids of the NS3 protease (NS3pro). Similar constructs have previously been shown to exhibit *cis* cleavage at the NS2B-NS3 junction when expressed either by recombinant vaccinia viruses (3) or in *in vitro* reticulocyte lysate translation systems employing microsomal membranes (17). As shown in Fig. 2*A*, expression of pTM.NS2B.NS3pro in a reticulocyte lysate supplemented with microsomal membranes (*lane 1*) clearly demonstrates processing of the 34-kDa NS2B.NS3pro precursor product into the expected 20-kDa NS3pro. In the absence of microsomal membranes, processing is less efficient, indicating the likely misfolding of the highly hydrophobic NS2B (Fig. 2*A*, *lane 2*). Given the hydrophobic nature of NS2B, with three predicted membrane-spanning domains (29), expression in association with NS3pro in *E. coli* would likely generate an insoluble product. However, Clum *et al.* (17) have shown that expression of the central conserved 40-amino acid hydrophilic domain of NS2B fused to NS3pro was sufficient for efficient co-factor activity. We generated a similar construct, pTM.CF40.NS3pro, and showed highly efficient processing of the expressed product *in vitro* in the absence of microsomal membranes (Fig. 2*A*, *lane 4*). Indeed, processing appeared complete with no precursor product apparent in the SDS-PAGE profile. It is possible that cleavage was mediated not by the *cis*-activity of NS3pro but via *trans*-cleavage by a contaminating protease. This possibility was addressed by mutation of one of the amino acids comprising the catalytic triad of NS3pro, $Ser^{135} \rightarrow Ala$ to generate pTM.CF40.NS3pro$^-$. Expression of this construct yielded the expected 32-kDa CF40.NS3pro precursor with no detectable cleavage (Fig. 2*A*, *lane 6*), demonstrating that the processing of pTM.CF40.NS3pro was due to the *cis*-activity of a catalytically active NS3pro. The additional species at ~28 kDa for both pTM.CF40.NS3pro and pTM.CF40.NS3pro$^-$ (Fig. 2*A*, *lanes 4* and *6*) was likely the product of internal initiation of translation at a downstream start codon.

Expression and Purification of NS3pro and CF40.NS3pro—To facilitate purification of *E. coli* expressed recombinant proteins, we used the pQE9 vector, which incorporates an amino-terminal hexahistidine tag allowing convenient purification by Ni^{2+} affinity chromatography. After the commencement of this project, Yusof *et al.* (18) reported a similar expression strategy

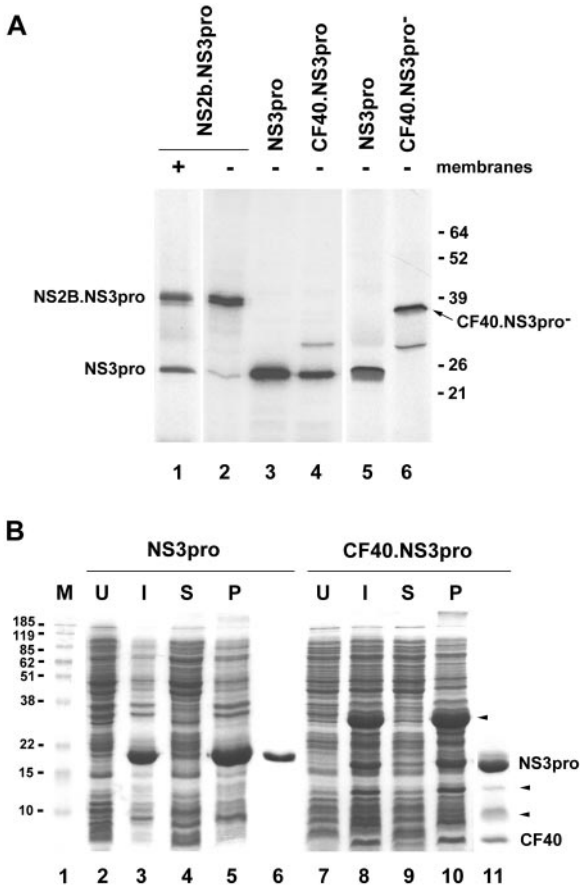

FIG. 2. ***In vitro* translation of NS2B/NS3 constructs and expression in *E. coli*.** A, pTM constructs encoding NS2B.NS3pro (*lanes 1* and *2*), NS3pro (*lanes 3* and *5*), CF40.NS3pro (*lane 4*), and CF40.NS3pro$^-$ (*lane 6*) were expressed *in vitro* in a coupled transcription/translation reaction, TnT. Incubations were carried out with or without canine pancreatic microsomal membranes as indicated, and products of *cis*-mediated cleavage were examined by SDS-PAGE and autoradiography. *B*, pQE9 recombinant constructs NS3pro and CF40.NS3pro were expressed in *E. coli*, and cell lysates were examined by SDS-PAGE and Coomassie Blue staining. The samples analyzed included protein molecular mass markers (*M*, *lane 1*), uninduced cell lysates (*U*, *lanes 2* and *7*), 1 mM induced cell lysates (*I*, *lanes 3* and *8*), the soluble fraction following lysis using a French press (*S*, *lanes 4* and *9*), and the insoluble pellet fraction (*P*, *lanes 5* and *10*). His-tagged recombinant products were purified by Ni^{2+} affinity chromatography from the soluble fractions of cell lysates (*lanes 6* and *11*).

and noted that although both NS3pro and an equivalent version of CF40.NS3pro were produced at high levels, the expressed proteins were found associated with insoluble inclusion bodies. Their solution was to purify urea-denatured recombinant protein from the insoluble pellet fraction of bacterial cell lysates and then refold the expressed products by successive dialysis. We investigated this approach but found that the refolding dialysis step consistently led to unacceptable levels of precipitation and poor recovery. Instead, we focused on optimizing expression conditions that favored the generation of soluble recombinant protein. Investigation of a range of parameters (data not shown) indicated that expression at 30 °C yielded low but acceptable levels of soluble protein (Fig. 2*B*, *lanes 4* and *9*) when purified by Ni^{2+} column affinity chromatography (Fig. 2*B*, *lanes 6* and *11*). This was particularly apparent for the CF40.NS3pro recombinant, which is suggestive of a chaperone-like function for CF40/NS2B in mediating the correct folding of NS3pro. Furthermore, although the majority of expressed recombinant in the insoluble pellet was uncleaved precursor (Fig. 2*B*, *arrowhead* in *lane 10*), the correct folding of

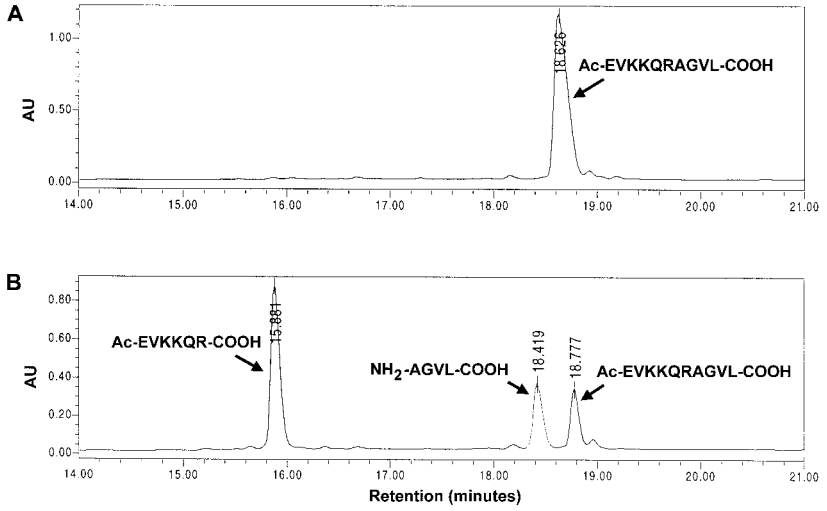

FIG. 3. **Reversed-phase HPLC analysis of the cleavage of Ac-EVKKQRAGVL-COOH by CF40.NS3pro.** *A*, HPLC profile of Ac-EVKKQRAGVL-COOH substrate alone. The retention time on the column is given in minutes, and peak detection was monitored at $A_{214\ nm}$. *B*, HPLC trace of the products of cleavage of the Ac-EVKKQRAGVL-COOH substrate after overnight incubation at 37 °C in the presence of 1 μM CF40.NS3pro.

the soluble form of the CF40.NS3pro complex was evidenced by its complete processing to the 20-kDa NS3pro and the 8-kDa co-factor domain (Fig. 2*B*, *lane 11*). Two additional intermediate species were also consistently identified in varying levels (indicated by *arrowheads* in Fig. 2*B*, *lane 11*). These were amino-terminally sequenced and shown to be truncated amino-terminal CF40.NS3pro products of auto-catalytic cleavage by CF40.NS3pro.

Characterization of Enzymatic Activity—To investigate whether CF40.NS3pro had proteolytic activity against small peptide substrates, we initially used buffer conditions similar to those reported for the hepatitis C virus NS3 protease (50 mM HEPES, pH 7.5, 70 mM NaCl, 20% glycerol, 0.1% Triton X-100). Reversed-phase HPLC was used to examine cleavage of the 10-residue peptide Ac-EVKKQRAGVL-COOH derived from the NS2B/NS3 site. Analytical HPLC (Fig. 3) showed the expected cleavage products Ac-EVKKQR-COOH and NH_2-AGVL-COOH, their identities being established by molecular mass determination through mass spectrometry and HPLC. The rate of cleavage of the decapeptide was slow. To optimize the enzyme processing conditions and to facilitate continuous monitoring of this reaction, we constructed the analogous chromogenic *para*-nitroanilide substrate Ac-EVKKQR-pNA corresponding to the P6-P1 segment amino-terminal to the NS2B-NS3 cleavage site but with a more reactive, hydrolytically cleavable, *para*-nitroanilide at the P1′ position. By monitoring the absorbance increase at 405 nm as a function of time, we were able to quantitatively compare the rates of processing of this substrate with Ac-RTSKKR-pNA, Ac-FAAGRK-pNA, and Ac-TTSTRR-pNA, corresponding to the NS2A/NS2B, NS3/NS4A, and NS4B/NS5 cleavage sites, respectively. We chose the most rapidly cleaved substrate (NS4B/5) to further examine the effects of diluents on substrate processing.

Effect of pH, Salt, Glycerol, and Detergents on Enzyme Activity—Using 1 μM purified CF40.NS3pro, we found that the substrate Ac-TTSTRR-pNA was cleaved most rapidly and most efficiently at a concentration of 500 μM, which was therefore used to optimize assay conditions. The pH dependence for enzyme processing was determined at a constant ionic strength (I = 50 mM) using various buffers with overlapping pH ranges between pH 5.5 and 11.5. These were MES (pH 5.5–7.0), MOPS (pH 6.5–8.0), Tris (pH 7.5–9.0), ethanolamine (pH 8.5–10.0), and CAPS (pH 10.0–11.5). The optimum pH for proteolytic processing was found to be 9.2, but above pH 9.5 the pNA substrate itself begins to undergo base-catalyzed hydrolysis in the absence of enzyme (Fig. 4*A*). At pH 9.0, base-catalyzed cleavage of pNA was negligible, whereas the enzyme was about five times more active in processing substrate than at a pH of 7.5. We therefore chose a 50 mM Tris buffer at pH 9.0 for investigating substrate cleavage.

Fig. 4*B* shows that increasing ionic strength has a significant effect on substrate processing, with the protease being susceptible to inhibition by salt at higher ionic strengths. This has also been observed for the hepatitis C NS3 protease. The minimum ionic strength (I) for 50 mM Tris at pH 9.0 was 10 mM; therefore this ionic strength was used in further work. Because NS3pro is thought to be membrane-associated, the effects of glycerol and detergents were also investigated to test their effect on enzyme efficiency. A titration experiment using glycerol indicated that optimal activity was obtained in the presence of 20% glycerol (Fig. 4*C*), with activity being improved about 1.3-fold over no glycerol. We also determined the effect of different zwitterionic and nonionic detergents on the enzymatic activity, and although Triton X-100, BRIJ-35, and CHAPS at 0.05–0.5% all increased activity, there were no significant differences between detergents (data not shown). For ease of handing, 1 mM CHAPS was subsequently used in cleavage experiments. Hence, our optimal buffer composition for substrate cleavage was 50 mM Tris, pH 9.0, 10 mM NaCl, 20% glycerol, and 1 mM CHAPS. The optimization of this simple *in vitro* assay for dengue virus NS3 protease activity in a 96-well format should prove invaluable for supporting not only structure-based drug design but also for high throughput screening of libraries of compounds for candidate lead inhibitors.

By analogy with the HCV NS3 protease where co-factor activity can be supplied in *trans* with a small 14-amino acid peptide derived from NS4A (30, 31), we had earlier proposed that an equivalent central hydrophobic 14-amino acid domain (^{70}GSSPILSITISEDG^{83}) within the previously identified 40-amino acid region of the flavivirus NS2B co-factor may be sufficient for activity (29). The availability of a sensitive *in vitro* assay now allowed us to test this hypothesis. A 13-residue peptide based on the sequence (NH_2-^{69}SGSSPILSITISE^{81}-COOH) was added as a putative co-factor to NS3pro, and the mixture was assayed. This peptide did not activate the protease, unlike similar short peptides, which were co-factors for HCV protease (data not shown). These data are supported by a recent report for the yellow fever virus NS3 protease that demonstrates that amino acids within the amino-terminal region of the 40-amino acid co-factor domain may be involved in additional charged interactions with NS3pro that are essential for activity (32). A requirement for these residues would further distinguish the flavivirus NS3 serine protease from its HCV counterpart.

Comparison of Peptide Substrates—The catalytic efficiency and specificity of the CF40.NS3pro protease was examined by

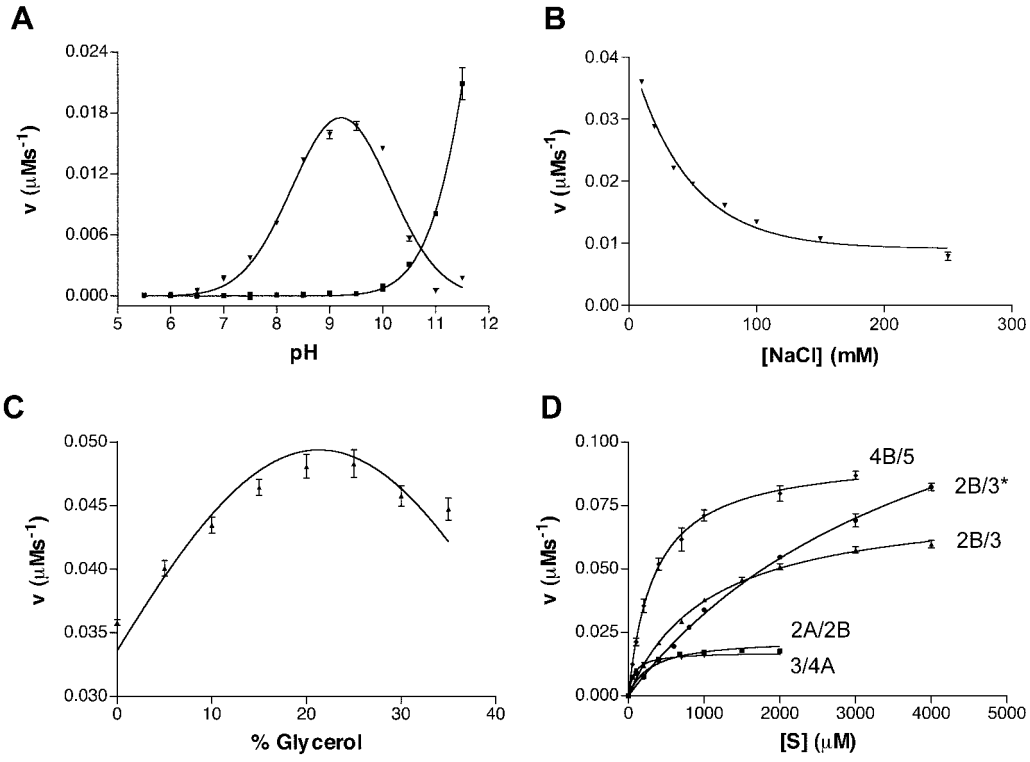

FIG. 4. **Characterization of the enzymatic properties of CF40.NS3pro.** *A*, pH dependence of CF40.NS3pro. Processing of substrate Ac-TTSTRR-pNA (500 μM) by CF40.NS3pro (1 μM) at constant ionic strength (I = 50 mM (NaCl)) using different pH buffers (50 mM MES, MOPS, Tris, ethanolamine, or CAPS) in the pH range of 5.5 to 11.5 (▼) compared with hydrolysis of the substrate under the same conditions in the absence of enzyme (■). *B*, effect of ionic strength; processing of substrate Ac-TTSTRR-pNA (500 μM) by CF40.NS3pro (1 μM) at pH 9.0 (50 mM Tris) in the presence of a varying NaCl concentration. *C*, dependence on glycerol concentration; processing of substrate Ac-TTSTRR-pNA (500 μM) by CF40.NS3pro (1 μM) at pH 9.0 (50 mM Tris) in the presence of a varying concentration of glycerol. *D*, K_m determination of pNA substrates based on cleavage sites NS2A/2B (■, 2A/2B), NS2B/3 (▲, 2B/3), NS3/4A (▼, 3/4A), NS4B/5 (♦, 4B/5) and a 10-residue peptide substrate based on the NS2B/3 cleavage site (●, 2B/3*). K_m was determined using CF40.NS3pro at 1.0 μM in 50 mM Tris, pH 9.0, 10 mM NaCl, 20% glycerol, 1 mM CHAPS.

measuring kinetic parameters for processing of the pNA substrate analogues of four hexapeptides corresponding to the P6-P1 residues amino-terminal to four cleavage sites (2A/B, 2B/3, 3/4A, 4B/5) within the polypeptide precursor. The rate of substrate hydrolysis and the Michaelis-Menten equilibrium constants are markedly sequence-dependent (Fig. 4*D*), with the sequences corresponding to the NS4B/NS5 and NS2B/3 cleavage sites being most rapidly cleaved. The rank order of k_{cat} for these pNA substrates is 4B/5 > 2B/3 ≫ 2A/2B ~ 3/4A (Table I). These residues have either Arg-Arg or Gln-Arg at the P2-P1 positions. On the other hand K_m varies in the order 2B/3 ≫ 4B/5 ≫ 2A/2B ~ 3/4A leading to a rank order of substrate efficiency or fitness as substrates (k_{cat}/K_m): 4B/5 > 3/4A > 2A/2B > 2B/3 (Table I). Interestingly the decapeptide Ac-EVKKQRAGVL-COOH, corresponding to the 2B/3 cleavage site, is processed less efficiently than the corresponding hexapeptide-pNA substrate Ac-EVKKQR-pNA (Table I).

Inhibition By Standard Serine Protease Inhibitors—The effect of standard protease inhibitors on substrate processing by CF40.NS3pro was also investigated. The percentage of cleavage in the presence of added inhibitors was determined as residual activity with respect to the control sample in the absence of inhibitors (Fig. 5). Aprotinin was shown to inhibit the enzyme (IC_{50} = 65 nM), whereas other standard serine protease inhibitors such as 4-(2-aminoethyl) benzenesulfonyl fluoride.hydrochloride and N-Tosyl-L-phenylalanine chloromethyl ketone showed only 20–30% inhibition at 500 μM and 1 mM, respectively. Other serine protease inhibitors for which no enzyme inhibition was found included soybean trypsin inhibitor (50 μM), 4-Amidinophenylmethanesulfonyl fluoride.hydrochloride (0.5 mM), phenylmethylsulfonyl fluoride (0.5 mM), leupeptin (0.5 mM), pepstatin A (0.1 mM), benzamidine (1 mM), and N-Tosyl-L-lysine chloromethyl ketone.hydrochloride (0.5 mM). The effect of divalent cations (Ca^{2+}, Mg^{2+}, and Mn^{2+}) was also investigated with the addition of 20 mM $CaCl_2$, 50 mM $MgCl_2$, or 50 mM $MnCl_2$ having no effect on dengue virus NS3 protease activity. The failure of 1 mM EDTA to inhibit the enzyme (data not shown), further confirmed that divalent cations are not critical for enzyme activity.

TABLE I
Kinetic parameters for the hydrolysis of synthetic peptide substrates by dengue CF40.NS3pro at 37 °C

Substrate	K_m	k_{cat}	k_{cat}/K_m
	μM	s^{-1}	$M^{-1}\ s^{-1}$
Ac-RTSKKR-pNA (2A/2B)	98 ± 8	0.019 ± 0.001	191 ± 13
Ac-EVKKQR-pNA (2B/3)	1079 ± 58	0.077 ± 0.002	72 ± 3
Ac-FAAGRK-pNA (3/4A)	78 ± 5	0.017 ± 0.001	219 ± 9
Ac-TTSTRR-pNA (4B/5)	346 ± 28	0.095 ± 0.002	275 ± 17
Ac-EVKKQRAGVL-OH	4239 ± 294	0.169 ± 0.007	40 ± 2

Expression, Purification, and Enzymatic Characterization of CF40.gly.NS3pro—SDS-PAGE analysis of the purified CF40.NS3pro fractions eluted from the Ni^{2+} affinity column revealed that the products of *cis* cleavage (His-CF40 and NS3pro) were not necessarily in equimolar proportions (Fig. 2*B*, *lane 11*) and therefore may not display optimal enzyme kinetics. As a consequence of cleavage within *E. coli*, the recombinant CF40.NS3pro complex was purified via binding of the His tag fused to the amino terminus of CF40. Varying levels of imidazole were shown, however, to preferentially elute the tightly but noncovalently bound NS3pro from the complex (data not shown). Mass spectrometry confirmed that we had not purified the CF40 and NS3pro components in equimolar quantities (data not shown). Our earlier modeling of the den-

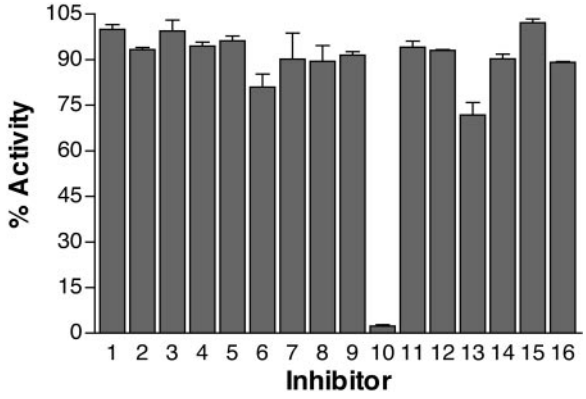

FIG. 5. **Inhibitor profile of CF40.NS3pro.** A range of inhibitors were tested for their activity against CF40.NS3pro. The test compounds were preincubated with 0.5 μM CF40.NS3pro for 10 min at 37 °C followed by the addition of the substrate Ac-TTSTRR-pNA at 500 μM. The reactions were performed in 50 mM Tris buffer, pH 9.0, 10 mM NaCl, 20% glycerol, 1 mM CHAPS in a final volume of 200 μl in a 96-well plate format. *Bar 1*, no inhibitor control; *bar 2*, soybean trypsin inhibitor (50 μM); *bar 3*, 4-Amidinophenylmethanesulfonyl fluoride.hydrochloride (0.1 mM); *bar 4*, 4-Amidinophenylmethanesulfonyl fluoride.hydrochloride (0.5 mM); *bar 5*, 4-(2-Aminoethyl) benzenesulfonyl fluoride.hydrochloride (0.1 mM); *bar 6*, 4-(2-Aminoethyl) benzenesulfonyl fluoride.hydrochloride (0.5 mM); *bar 7*, phenylmethylsulfonyl fluoride (0.5 mM); *bar 8*, leupeptin (0.1 mM); *bar 9*, leupeptin (0.5 mM); *bar 10*, aprotinin (3 μM); *bar 11*, pepstatin A (0.1 mM); *bar 12*, benzamidine (1 mM); *bar 13*, N-Tosyl-L-phenylalanine chloromethyl ketone (TPCK) (1 mM); *bar 14*, N-Tosyl-L-lysine chloromethyl ketone.hydrochloride (TLCK) (0.5 mM); *bar 15*, Me_2SO (5%); *bar 16*, EDTA (1 mM).

gue virus NS3 protease complexed with its co-factor (29) indicated that the carboxyl terminus of the co-factor was likely to be in close proximity to the amino terminus of NS3pro, suggesting the possibility of incorporating a short linker between the two domains that would not disrupt the structural integrity of the complex. So, to remedy the problems associated with purifying a noncovalently bound complex, we engineered a new construct that expressed a catalytically active NS3pro fused to CF40 via a noncleavable, flexible nonapeptide ($Gly_4SerGly_4$) linker, the fusion protein designated as CF40.gly.NS3pro (Fig. 1*B*). Expression of this construct resulted in substantially higher levels of recombinant protein being found in the soluble fraction of the bacterial cell lysate (Fig. 6*A*, *lane 4*) with yields of purified CF40.gly.NS3pro (Fig. 6*A*, *lane 6*) approaching 50 mg/L of culture.

Using 1 μM purified CF40.gly.NS3pro and 500 μM Ac-TTSTRR-pNA, the pH dependence for enzyme processing was determined at a constant ionic strength (I = 50 mM) using the same buffers as described in the previous section with overlapping pH ranges between pH 5.5 and 11.5. The optimum pH for proteolytic processing was again found to be pH 9.2 (Fig. 6*B*). By comparison the glycine-linked conjugate enzyme CF40.gly.NS3pro was significantly more catalytically active (about 4-fold) than the CF40.NS3 construct under the same conditions (Fig. 6*B*). The enzyme kinetics of CF40.gly.NS3pro were investigated using the same pNA substrates described above and the same reaction conditions that had been optimized for CF40.NS3pro. The results presented in Fig. 6*C* and Table II indicate that although the binding affinities (K_m) of the substrates for CF40.gly.NS3pro were similar to those for CF40.NS3pro, the catalytic rates (k_{cat}) were significantly higher, leading to higher overall proteolytic efficiencies (k_{cat}/K_m) for the covalently linked (noncleavable) form. In summary, the data in Fig. 6 (*B* and *C*) demonstrate that the glycine-linked enzyme is the more active form. We attribute this to the absence of cleavage between co-factor and protease domains in CF40.gly.NS3pro.

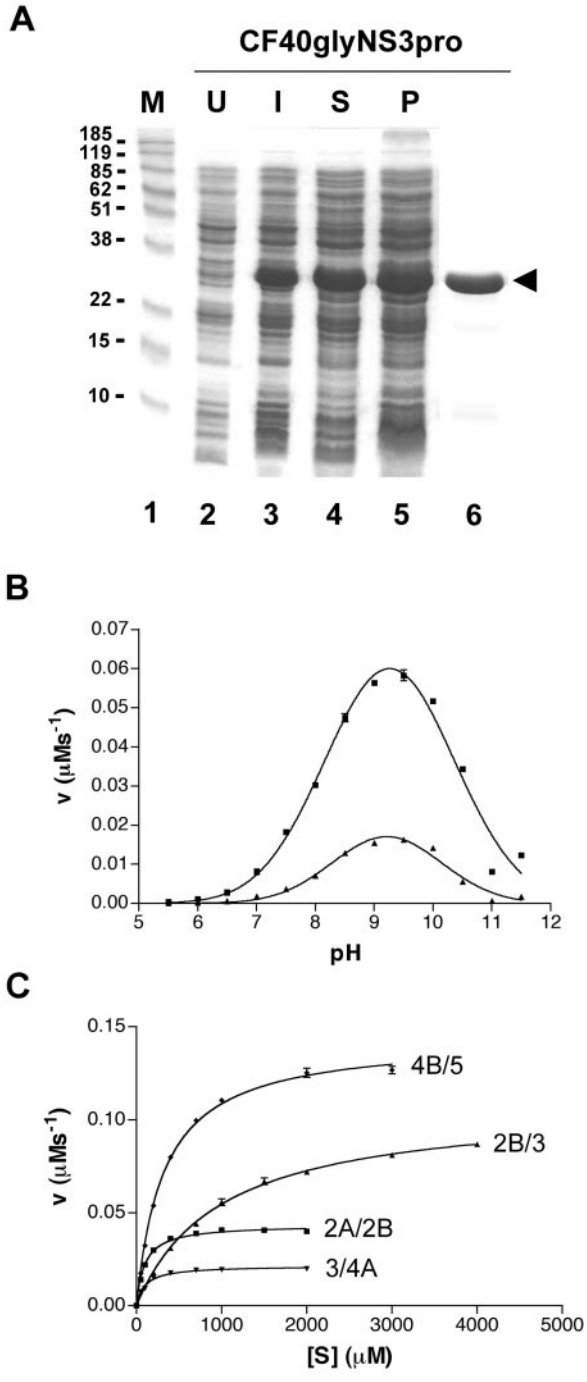

FIG. 6. **Expression of CF40.gly.NS3pro in *E. coli* and characterization of its enzymatic properties.** *A*, the pQE9 recombinant construct CF40.gly.NS3pro (see Fig. 1*B*) was expressed in *E. coli*, and cell lysates were examined by SDS-PAGE and Coomassie Blue staining. Samples analyzed include protein molecular mass markers (*M*, *lane 1*), uninduced cell lysate (*U*, *lane 2*), 1 mM induced cell lysate (*I*, *lane 3*), the soluble fraction following lysis using a French press (*S*, *lane 4*), and the insoluble pellet fraction (*P*, *lane 5*). His-tagged recombinant products were purified by Ni^{2+} affinity chromatography from the soluble fraction after cell lysis using a French press (*lane 6*). *B*, comparison of the pH dependence of CF40.NS3pro (▲) and CF40.gly.NS3pro (■). Processing of substrate Ac-TTSTRR-pNA (500 μM) by enzyme (1 μM) at constant ionic strength (I = 50 mM (NaCl)) using different pH buffers (50 mM MES, MOPS, Tris, ethanolamine, or CAPS) in the pH range of 5.5–11.5. *C*, purified fractions eluted from the Ni^{2+} affinity column were concentrated in a Centricon-10 column, and the enzymatic properties of a 1.0 μM preparation were analyzed. K_m determination was made with pNA substrates based on cleavage sites NS2A/2B (■, 2A/2B), NS2B/3 (▲, 2B/3), NS3/4A (▼, 3/4A), and NS4B/5 (♦, 4B/5). The reaction conditions were as described for CF40.NS3pro, 50 mM Tris, pH 9.0, 10 mM NaCl, 20% glycerol, 1 mM CHAPS.

TABLE II
Kinetic parameters for the hydrolysis of synthetic peptide substrates by dengue CF40.gly.NS3pro at 37 °C

Substrate	K_m	k_{cat}	k_{cat}/K_m
	μM	s^{-1}	$M^{-1}\ s^{-1}$
Ac-RTSKKR-pNA (2A/2B)	96 ± 7	0.087 ± 0.001	903 ± 56
Ac-EVKKQR-pNA (2B/3)	984 ± 40	0.216 ± 0.002	220 ± 6
Ac-FAAGRK-pNA (3/4A)	100 ± 9	0.043 ± 0.001	425 ± 30
Ac-TTSTRR-pNA (4B/5)	326 ± 10	0.288 ± 0.001	883 ± 22

TABLE III
Inhibitors of dengue NS3 serine protease

	Inhibitor	K_i
		μM
1	Ac-FAAGRR-αketo-SL-$CONH_2$	47 ± 3
2	Ac-TTSTRR-αketo-SL-$CONH_2$	220 ± 55
3	Ac-TTSTRR-αketo-GTGN-$CONH_2$	368 ± 47
4	Ac-FAAGRR-CHO	16 ± 3

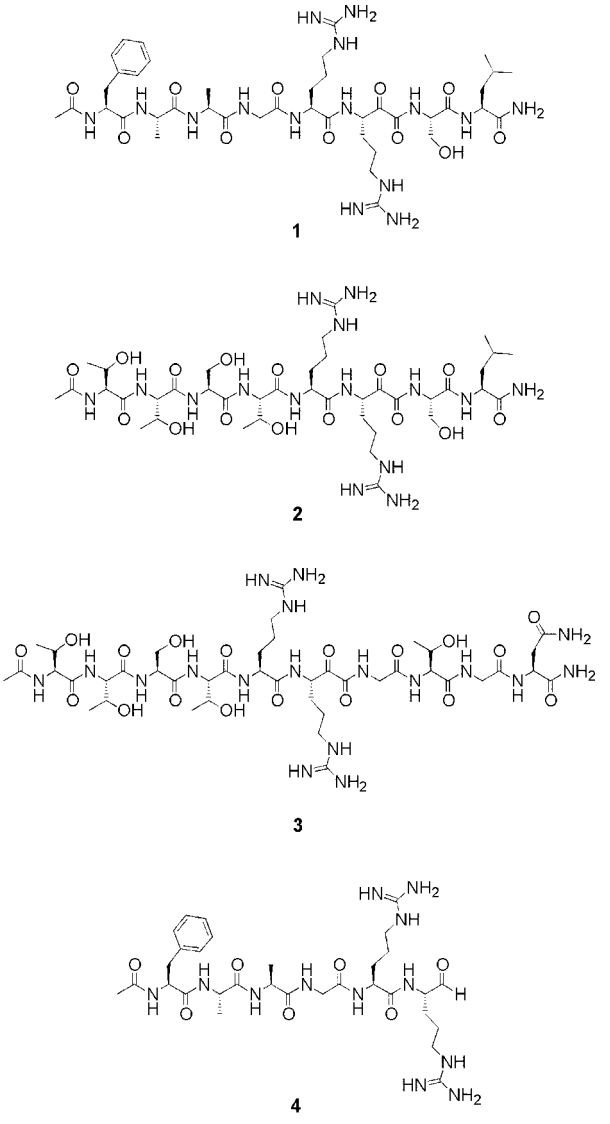

FIG. 7. **Dengue virus NS3pro peptide inhibitors.** Inhibitors were based on the dengue virus type 2 NS3/4A (*structures 1* and *4*) and NS4B/5 (*structures 2* and *3*) cleavage sites and synthesized as described under "Experimental Procedures."

Synthetic Peptide Inhibitors—Peptidic α-keto amide inhibitors have been well characterized as reversible competitive inhibitors for other serine proteases (33, 34), and most recently keto amides were shown to be potent inhibitors of the closely related HCV NS3 protease (35, 36). Fig. 7 shows several peptides that were constructed as prospective inhibitors of CF40.gly.NS3pro. Compound **1** was based on the P6-P2′ residues of the 3/4A polypeptide cleavage sequence. Compound **2** contains the P6-P2′ residues of the 4B/5 sequence, whereas compound **3** has P6-P4′ residues of the 4B/5 sequence. Compound 1 was more potent (~5-fold) than compounds **2** and **3** (Table III). All three compounds feature an α-keto amide "transition state isostere" in place of the cleavable amide bond. Lineweaver-Burk plots had the same ordinate intercept in the presence or absence of inhibitor, indicating that the mechanism was competitive (data not shown). Although the pH optimum for the protease was pH 9, the assay for peptide inhibitors was performed using CF40.gly.NS3 in 50 mM HEPES at more physiologically relevant conditions (pH 7.5). The α-keto amide inhibitors were found (37) to be unstable at pH 9 (data not shown). When the cleavable amide bond and residues P1′-P2′ are removed from compound **1** and replaced with a carboxyl-terminal aldehyde (*e.g.* 4), comparable inhibitory potency was observed (Table III). The most potent inhibitors from this series were **1** and **4**, consistent with the 3/4A site pNA analogue having the lowest K_m.

DISCUSSION

Sequence alignment studies had previously indicated that NS3pro would be structurally similar to trypsin-like serine proteases, and this has been largely borne out by a recent crystal structure of the free enzyme (38). However, unlike trypsin, NS3pro has a marked preference for basic residues at P2 and P1 in its peptide substrates in the vicinity of the cleavage site. We considered that this unusual requirement might provide an excellent basis for design of selective inhibitors for this enzyme and, because of the essential nature of the protease to viral replication, a possible basis for design of antiviral agents. Toward this goal, the present work has examined enzymatic properties of the recombinant NS3 protease (NS3pro) from the dengue virus, defined in a preliminary way its enzymatic activity, identified and overcome difficulties with autocatalytic cleavage of the co-factor from the protease, evaluated a series of short peptide substrates derivatized for spectrophotometric detection using a *para*-nitroaniline chromophore, and taken the first steps toward inhibitor development.

We found that, like other flavivirus proteases, NS3pro requires a co-factor from the NS2B region for proteolytic activity. Previous modeling and deletion studies had suggested that a sequence of 40 amino acids from NS2B would likely contain the requisite co-factor domain (16) and that a central core of 14 predominantly hydrophobic residues were thought to define the essential co-factor (29). Although this is a similar situation to the hepatitis C virus NS3 protease, unlike HCV we find that (i) solutions of NS3pro and peptide substrate alone fail to lead to proteolytic activity and (ii) addition of a synthetic 13-residue peptide corresponding to the putative co-factor did not lead to proteolysis (data not shown). However, when the dengue virus NS3 protease was co-expressed with the 40-residue co-factor sequence tethered to the amino terminus, substrate cleavage was observed in *cis* and in *trans*. Homology modeling (29) had previously suggested to us that this might be the case because the co-factor appears to be required to thread through a narrow channel of NS3pro for structural stability and therefore probably requires simultaneous folding of enzyme and co-factor to lead to correctly bound co-factor for productive proteolysis.

Our initial work with NS3pro alone showed negligible processing of small pNA peptide substrates. When co-expressed with co-factor (CF40.NS3pro), the enzyme demonstrated some proteolytic activity (Table I) by cleaving small peptide substrates, but mass spectrometry and reversed-phase HPLC suggested that this enzyme-co-factor adduct was unstable in the presence of protease, autocatalytically cleaving itself at the CF40.NS3pro junction. This was confirmed when the kinetic properties of the enzyme improved (Table II *versus* Table I) for a more stable co-factor-protease construct (CF40-nonapeptide-NS3pro) corresponding to the protease fused to the 40-residue co-factor by a flexible nonapeptide linker (Gly_4-Ser-Gly_4). This linker is not prone to enzymatic cleavage and thus prevents enzymatic separation of co-factor from protease. These observations are in accordance with an equilibrium in the case of CF40.NS3pro between intact and cleaved adduct, and the parameters obtained for this construct are similar to those recently reported for a similar construct (18). Consequently, we propose that a noncleavable linker between co-factor and protease, described for the first time herein, is needed for optimal enzymatic activity.

By implication it would appear that NS2B functions as a molecular chaperone in assisting the folding of NS3pro to an active conformation that is presumably subtly different from that reported in the recent crystal structure of the isolated protease without co-factor (33). Other serine proteases (*e.g.* α-lytic protease, subtilisin) are known to require a pro-region like NS2B for productive folding that leads to protease activity. Once folding is completed, the pro-region is dispensable and does not form a component of the active enzyme. In the case of the hepatitis C virus NS3 protease, there was also a dependence on Zn^{2+} because of its structural role in stabilizing the folding of the protease. Studies here with EDTA and divalent cations confirmed our previous suggestion from homology modeling (29) that metal ions are not important for protease activity. This is supported by the crystal structures of NS3pro (38, 39), which contained no metal ions.

We have also reported the first demonstration of cleavage site preferences for NS3pro. The kinetic substrate profiles were obtained using hexapeptide substrates modified as chromogenic pNA derivatives rather than the more tedious approach using recombinant substrates. The observed cleavage efficiency and selectivity profile (Tables I and II) for the four substrates examined may provide useful clues for inhibitor development. Interestingly, the longer decapeptide substrate was not cleaved as efficiently as the pNA substrates, whereas for hepatitis C virus NS3 protease the longer peptides are more effective substrates (31). The crystal structure of free NS3pro suggests that there may not be an essential requirement for amino acids in the substrate beyond P2′ on the carboxyl side of the scissile bond for substrate binding (38).

Initial attempts here to investigate the inhibition of NS3pro have revealed that this protease is not inhibited by standard serine protease inhibitors (Fig. 5) except for aprotinin, which is a potent inhibitor at submicromolar concentrations. However, this inhibitor is a large protein and probably denies substrate access to the protease active site by enveloping the enzyme. Table III shows some preliminary indications that small molecule inhibitors, based upon the peptide substrates reported herein, may be able to be developed as inhibitors of NS3pro. Although the indicated compounds are only inhibitors at micromolar concentrations, we can expect to improve upon this potency through structural optimization and with better carboxyl-terminal isosteres that permit more effective interaction with catalytic residues of this serine protease. Because of the critical and unusual requirement of dibasic residues for substrates of this flavivirus NS3 protease, there would appear to be good prospects for the design of protease inhibitors that selectively inactivate NS3pro without inactivating essential proteases for physiological function.

Acknowledgment—We thank Jodie Robinson for excellent technical assistance.

REFERENCES

1. Jacobs, M. G., and Young, P. R. (1998) *Curr. Opin. Infect. Dis.* **11,** 319–324
2. Chambers, T. J., Hahn, C. S., Galler, R., and Rice, C. M. (1990) *Annu. Rev. Microbiol.* **44,** 649–688
3. Falgout, B., Pethel, M., Zhang, Y. M., and Lai, C. J. (1991) *J. Virol.* **65,** 2467–2475
4. Wengler, G., and Wengler, G. (1991) *Virology* **184,** 707–715
5. Li, H. T., Clum, S., You, S. H., Ebner, K. E., and Padmanabhan, R. (1999) *J. Virol.* **73,** 3108–3116
6. Bazan, J. F., and Fletterick, R. J. (1989) *Virology* **171,** 637–639
7. Bazan, J. F., and Fletterick, R. J. (1990) *Semin. Virol.* **1,** 311–322
8. Gorbalenya, A. E., Donchenko, A. P., Koonin, E. V., and Blinov, V. M. (1989) *Nucleic Acids Res.* **17,** 3889–3897
9. Chambers, T. J., Weir, R. C., Grakoui, A., McCourt, D. W., Bazan, J. F., Fletterick, R. J., and Rice, C. M. (1990) *Proc. Natl. Acad. Sci. U. S. A.* **87,** 8898–8902
10. Preugschat, F., Yao, C. W., and Strauss, J. H. (1990) *J. Virol.* **64,** 4364–4374
11. Preugschat, F., Lenches, E. M., and Strauss, J. H. (1991) *J. Virol.* **65,** 4749–4758
12. Falgout, B., and Markoff, L. (1995) *J. Virol.* **69,** 7232–7243
13. Speight, G., Coia, G., Parker, M. D., and Westaway, E. G. (1988) *J. Gen. Virol.* **69,** 23–34
14. Nowak, T., Farber, P. M., Wengler, G., and Wengler, G. (1989) *Virology* **169,** 365–376
15. Stadler, K., Allison, S. L., Schalich, J., and Heinz, F. X. (1997) *J. Virol.* **71,** 8475–8481
16. Falgout, B., Miller, R. H., and Lai, C. J. (1993) *J. Virol.* **67,** 2034–2042
17. Clum, S., Ebner, K. E., and Padmanabhan, R. (1997) *J. Biol. Chem.* **272,** 30715–30723
18. Yusof, R., Clum, S., Wetzel, M., Krishna Murthy, H. M., and Padmanabhan, R. (2000) *J. Biol. Chem.* **275,** 9963–9969
19. Leung, D., Abbenante, G., and Fairlie, D. P. (2000) *J. Med. Chem.* **43,** 305–341
20. Seife, C. (1997) *Science* **277,** 1602–1603
21. Ripka, A. S., and Rich, D. H. (1998) *Curr. Opin. Chem. Biol.* **2,** 441–452
22. Kempf, D. J., and Sham, H. L. (1996) *Curr. Pharm. Des.* **2,** 225–246
23. West, M. L., Fairlie, D. P. (1995) *Trends Pharmacol. Sci.* **16,** 67–75
24. Abbenante, G., Leung, D., Bond, T., and Fairlie, D. P. (2001) *Lett. Pept. Sci.*, in press
25. Webb, T. R., Reiner, J. E., Tamura, S. Y., Ripka, W. C., and Dagnino, R., Jr. (May 7, 1996) U.S. Patent 5,514,777
26. Ripka, W. C., Webb, T. R., Dagnino, R., Jr., Nutt, R. F., Reiner, J. E., and Tamura, S. Y. (March 24, 1998) U.S. Patent 5,731,413
27. Tamura, S. Y., Semple, J. E., Ardecky, R. J., Leon, P., Carpenter, S. H., Yu, G., Shamblin, B. M., Weinhouse, M. I., Ripka, W. C., and Nutt, R. F. (1996) *Tetrahedron Lett.* **37,** 4109–4112
28. Semple, J. E., Minami, N. K., Tamura, S. Y., Brunck, T. K., Nutt, R. F., and Ripka, W. C. (1997) *Bioorg. Med. Chem. Lett.* **7,** 2421–2426
29. Brinkworth, R. I., Fairlie, D. P., Leung, D., and Young, P. R. (1999) *J. Gen. Virol.* **80,** 1167–1177
30. Steinkuhler, C., Tomei, L., and De Francesco, R. (1996) *J. Biol. Chem.* **271,** 6367–6373
31. Steinkuhler, C., Urbani, A., Tomei, L., Biasiol, G., Sardana, M., Bianchi, E., Pessi, A., and De Francesco, R. (1996) *J. Virol.* **70,** 6694–6700
32. Droll, D. A., Murthy, H. M. K., and Chambers, T. J. (2000) *Virology* **275,** 335–347
33. Edwards, P. D., and Bernstein, P. R. (1994) *Med. Res. Rev.* **14,** 127–194
34. Babine, R. E., and Bender, S. L. (1997) *Chem. Rev.* **97,** 1359–1472
35. Han, W., Hu, Z., Jiang, X., and Decicco, C. P. (2000) *Bioorg. Med. Chem. Lett.* **10,** 711–713
36. Bennett, J. M., Campbell, A. D., Campbell, A. J., Carr, M. G., Dunsdon, R. M., Greening, J. R., Hurst, D. N., Jennings, N. S., Jones, P. S., Jordan, S., Kay, P. B., O'Brien, M. A., King-Underwood, J., Raynham, T. M., Wilkinson, C. S., Wilkinson, T. C., and Wilson, F. X. (2001) *Bioorg. Med. Chem. Lett.* **11,** 355–357
37. Leung, D. (2001) *Studies of Serine and Cysteine Protease Inhibitors*. Ph.D. Dissertation, University of Queensland, Brisbane, Australia
38. Murthy, H. M., Clum, S., and Padmanabhan, R. (1999) *J. Biol. Chem.* **274,** 5573–5580
39. Murthy, H. M., Judge, K., DeLucas, L., and Padmanabhan, R. (2000) *J. Mol. Biol.* **301,** 759–767

Activity of Recombinant Dengue 2 Virus NS3 Protease in the Presence of a Truncated NS2B Co-factor, Small Peptide Substrates, and Inhibitors

Donmienne Leung, Kate Schroder, Helen White, Ning-Xia Fang, Martin J. Stoermer, Giovanni Abbenante, Jennifer L. Martin, Paul R. Young and David P. Fairlie

J. Biol. Chem. 2001, 276:45762-45771.
doi: 10.1074/jbc.M107360200 originally published online October 1, 2001
